Quasi-static continuum model of octopus arm configuration under water

Amirreza F.Golestaneh [1]
mpeafg@nus.edu.sg

Gianmarco Mengaldo [1]
mpegim@nus.edu.sg

Jonathan Lim Ming En [1]
e0310473@u.nus.edu

Adamya Dhaker Singh [2]
ADAMYASI001@e.ntu.edu.sg

Chandraveer Saran [3]
f20180541@pilani.bits-pilani.ac.in

Cecilia Laschi [1]
mpeclc@nus.edu.sg

1: Dept. of mechanical engineering, National University of Singapore, Singapore.
2: School of Mechanical and Aerospace Engineering, Nanyang Technological University, Singapore.
3: Dept. of mechanical engineering, Birla Institute of Technology and Science, Pilani, India.

The current work aims to present a quasi-static model of a soft robot arm configuration, inspired by octopus arm. The arm is assumed under the water and hence the main goal is to study the impacts of hydrostatic force, tangential and normal forces of the water imposed to the arm as the environmental interactions, where the arm is driven by tensions of two longitudinal cables along the arm, as the actuators. The arm is modeled as a two-dimensional continuum robot by implementation of Cosserat theory of rods, where the cross section of the rod is capable of rigid rotation such that the it is not locally constrained to be normal to the direction of the rod at any point along the rod. This is in fact of significant importance to modeling of hollow rods and rods with large bending deformations. Unlike the standard Cosserat theory of rods, the cross section of the rod undergoes planar deformation, avoiding any off-plane warping of the cross section. It is notable that this planar deformation of the rod cross section plays an essential role in preserving the volume of the rod locally. In line with the main goal, a constitutive model is used for the material of the octopus arm to model the characteristic behavior of that material as it undergoes internal and external loadings.

The two-dimensional (2D) configuration of the octopus arm is parametrized by curve length s of centerline of undeformed straight rod, using Cosserat theory:

$$[0.0, L] \ni s \longmapsto \mathbf{r}(s)$$
$$s \longmapsto \mathbf{b}(s), \quad (1)$$

where $\mathbf{r}(s)$ parametrizes the centerline of the rod and $\mathbf{b}(s)$ is the unit vector *director* along the cross section such that the other unit director is defined as $\mathbf{a}(s) = \mathbf{b}(s) \times \mathbf{k}$ for $\mathbf{k}$ being the unit vector normal to the plane. Let decompose the tangent vector $\mathbf{t}(s)$:

$$\mathbf{t}(s) \doteq \mathbf{r}'(s) = \nu(s)\mathbf{a}(s) + \eta(s)\mathbf{b}(s), \quad (2)$$

where $()' \doteq \frac{\partial()}{\partial s}$ and $\nu(s) and \eta(s)$ are respectively normal, shear strains. It is notable that $\mu(s) \doteq \theta'(s)$ is the bending strain of the arm, where $\mathbf{a}(s) = \cos(\theta)\mathbf{e}_1 + \sin(\theta)\mathbf{e}_2$ and

accordingly for $\mathbf{b}(s)$. The configuration of undeformed straight conical rod is determined by:

$$\mathbf{X}(\mathbf{s}) = s\,\mathbf{e}_1 \pm X_2(s)\mathbf{e}_2, \quad (3)$$

where $X_2(s)$ similarly denotes the radius $R(s)$ of undeformed rod and $\mathbf{e}_1, \mathbf{e}_2$ are planar Cartesian basis. The deformed rod is parametrized as:

$$\mathbf{x}(s) = \mathbf{r}(s) \pm x_2(X_2(s), s)\mathbf{b}(s), \quad (4)$$

where $x_2(X_2(s), s) = \beta(s)X_2(s)$ such that $\beta(s) = \frac{\partial x_2(s)}{\partial X_2(s)}$ is the cross sectional normal strain of rod along $\mathbf{b}(s)$ director. Here similar ideas for point force $\mathbf{n}_i(s)$ at $s = L$ and distributed force $\mathbf{n}_i^D(s)$ of the cable tensions T_i for $i \in 1,2$ are adopted from [1]:

$$\mathbf{n}_i(L) = -T_i\,\mathbf{t}_{ci}(L), \quad i \in \{1,2\} \quad (5)$$

$$\mathbf{n}_i^D(s) = \int_s^L T_i\frac{\mathrm{d}\mathbf{t}_{ci}(\xi)}{\mathrm{d}\xi}\mathrm{d}\xi, \quad (6)$$

where $\mathbf{t}_{ci}$ is the unit tangent vector to the cable $\mathbf{r}_{ci}(s) = \mathbf{r}(s) \pm y_c(s)\beta(s)\mathbf{b}(s)$ and $y_c(s)$ is the distance of cable i from the centerline of straight rod.

A quasi-static analysis is implemented here to model the impacts of the environmental fluid on kinematics of the arm, in which the arm deformed configuration is studied statically at every instant of incremental tension of the cables. Therefore, a flow of a viscous fluid with quadratic velocity profile $\mathbf{v}_t(s, y)$ of normal distance $y \in [0, h_\infty]$ from the arm surface, is assumed over the arm, which satisfies the no-slip condition on the arm surface and monotonically increases to its maximum at normal distance h_∞ from the arm:

$$\mathbf{v}_t(s, y) = v_{t\infty}(s)\left[-\left(\frac{y}{h_\infty}\right)^2 + \frac{2y}{h_\infty}\right]\mathbf{u}_t(s), \quad (7)$$

where $\mathbf{u}_t(s)$ is the unit tangent vector to the arm surface, $v_{t\infty}(s) = \mathbf{v}_\infty \cdot \mathbf{u}_t(s)$ and $\mathbf{v}_\infty = v_\infty\mathbf{e}_1$ is the tangential component of free-stream velocity of flow. The principle of linear momentum for a steady state flow is applied separately over an infinitesimal control volume of fluid on surfaces of the arm on both sides of the centerline to compute the

resultant forces imposed by the change of flow momentum in tangential and normal directions to the arm. This normal resultant force of fluid includes the resultant hydrostatic force (Buoyant force), $\mathbf{F}_{Hyd}(s)$, versus the weight of the arm:

$$d\mathbf{F}_t^L(s) = -\left(V_{n_{in}}^2(s) + 2V_{t_{in}}(s)V_{n_{in}}(s)\right)\pi\rho_w\beta X_2 ds\mathbf{u}_t(s), \tag{8}$$

$$d\mathbf{F}_n^L(s) = -\left[d\mathbf{F}_{Hyd}(s) + \pi\rho_w\beta X_2 V_{n_{in}}^2(s)ds\right]\mathbf{u}_n(s), \tag{9}$$

$$d\mathbf{F}_n^R(s) = -d\mathbf{F}_{Hyd}(s)\mathbf{u}_n(s), \tag{10}$$

where the superscripts L and R respectively denote the surface of arm on the left and right hand sides of centerline and subscripts t, n and in respectively denote tangential and normal directions to the arm and entering flow velocities to the control volume.

The resultant internal contact force $\mathbf{n}^c$ and moment $\mathbf{m}^c$ convey the external loadings to constitutive behavior of the arm as:

$$\mathbf{n}^c(s) = (N(s)\mathbf{a}(s) + H(s)\mathbf{b}(s))\,A(s), \tag{11}$$

$$\mathbf{m}^c(s) = M(s)A(s)\mathbf{k}, \tag{12}$$

where $N(s)$, $H(s)$ and $M(s)$ respectively denote normal, shear and bending stresses and $A(s) = \pi(\beta(s)X_2(s))^2$ is cross sectional area of rod. A hyperelastic strain energy is assumed for constitutive behavior of the arm material with $C_1(s)$, $C_2(s)$ and $C_3(s)$ coefficients:

$$\hat{W}(\nu,\eta,\mu,s) = C_1(s)(\nu-\nu_o)^2 + C_2(s)(\eta-\eta_o)^2 + C_3(s)(\mu-\mu_o)^2. \tag{13}$$

Then from required conditions for any constitutive model:

$$\hat{N}(s) = C_1(\nu(s) - 1), \tag{14a}$$

$$\hat{H}(s) = C_2\eta(s), \tag{14b}$$

$$\hat{M}(s) = C_3\mu(s), \tag{14c}$$

where $C_1, C_2, C_3 > 0$.

The equilibrium equations of forces and moments generate three nonlinear ordinary differential equations (ODEs) of normal $\nu(s)$, shear $\eta(s)$ and bending $\mu(s)$ strains. Another ODE is extracted for cross sectional normal strain $\beta(s)$ from the constraint of locally volume preserved deformation of the arm. This constraint is aligned with the biological behavior of the muscular hydrostats like octopus arm, for which the stiffness of the hydrostat is directly induced by the incompressibility of the tissues:

$$\frac{\partial v(s)}{\partial V(s)} = \det(\mathbf{F}(s)) = 1, \tag{15}$$

where V and v are respectively volumes of undeformed and deformed arms and deformation gradient of the bulk rod is defined by tensor product $\otimes$ for $\alpha \in 1, 2$:

$$\mathbf{F}(s) = \frac{\partial\mathbf{x}(s)}{\partial X_\alpha(s)} \otimes \mathbf{e}_\alpha. \tag{16}$$
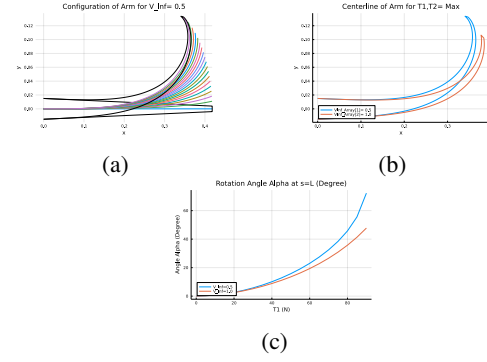

Fig. 1: Arm configurations.

The system of four nonlinear ODEs are then solved using the boundary conditions (BCs) for the fixed support arm: $\nu_o = \beta_o = 1$, $\eta_o = \mu_o = 0$ and $\beta_o' = 0$.

Fig.1a shows the deformed configurations of the arm for various incrementally increased tensions T_1 of the cable for free-stream velocity $v_\infty = 0.5\ m/s$. It is of interest that as the arm is deformed more for higher tensions of the cable the cross section of the arm at the tip $s = L$ is more rotated. That means the cross section is perpendicular to the direction of the centerline in undeformed straight arm such that the angle between normal unit vector $\mathbf{a}(L)$ of the cross section and the tangent vector $\mathbf{t}(L)$ of the centerline is $\alpha(L) = 0.0°$, where this angle gradually rises up to the large angle $\alpha(L) = 72.25°$ for highest cable tension (see the blue plot in Fig.1c). Recall that in the current model the arm undergoes cross sectional normal strain $\beta(s)$, which means the radius of the arm cross section adjusts locally along the deformed arm such that the deformation of the arm is locally volume preserved. This is aligned with the biological behavior of the octopus arm, for which the stiffness is directly caused by the incompressibility of the tissues.

Fig.1b asserts that the deformation of the arm, which is imposed to a fixed tension of the cable T_1, is reduced for higher free-stream flow velocity. That consequently proceeds to the smaller cross sectional rotation of the arm, as shown for the tips at $s = L$. The variation of the rotation angle $\alpha(s)$ of the arm cross section for two free-stream velocities of flow was plotted along the arm in Fig.1c. The rotation angle grows along the arm, while it is locally smaller for higher free-stream velocity of flow, since the arm undergoes smaller deformation.

In general, the results explain that it is of significant importance to account for the influences of the surrounding fluid in kinematic modeling of the octopus arm under the water, while implementation of rigid rotation and planar deformation of the arm cross section enhance the precision of the model.

REFERENCES

[1] Michele Giorelli, Federico Renda, Marcello Calisti, Andrea Arienti, Gabriele Ferri, and Cecilia Laschi. A two dimensional inverse kinetics model of a cable driven manipulator inspired by the octopus arm. In *2012 IEEE International Conference on Robotics and Automation*, pages 3819–3824, 2012.